ORIGINAL ARTICLE

Multi-response optimization of TIG dissimilar welding of AISI 1008 mild steel and AISI 316 stainless steel using grey-based Taguchi method

Okwudili Simeon Ogbonna[1] · Stephen Akinlabi Akinlabi[2] · Nkosinathi Madushele[1] · Olawale Samuel Fatoba[1] · Esther Titilayo Akinlabi[2]

Abstract

This article presents a reliable method of multi-performance characteristics optimization of TIG dissimilar welding of mild steel and stainless steel. Grey-integrated Taguchi optimization approach was adopted for the optimization of the welding process parameters such as the welding current, the welding voltage and the gas flow rate for multi-performance characteristics such as the ultimate tensile strength, yield strength, percentage elongation and Vickers microhardness of the fusion zone. L_9 Taguchi orthogonal array was employed with three process parameters all at three levels. The welding current was the most significant process parameter for the multi-performance characteristics of the weld joint. The optimal setting for the multi-performance characteristics of the weld joint was obtained as welding current at level 1 (110 A), welding voltage at level 1 (11 V) and gas flow rate at level 3 (18 l min^{-1}). The corresponding response variables at the optimal setting were ultimate tensile strength, yield strength, percentage elongation and Vickers microhardness of 493.29 MPa, 395.38 MPa, 31.35% and 390.52 HV respectively. These values are all found to be higher than the values obtained at the initial settings. This shows that grey-integrated Taguchi optimization is an effective method in multi-performance characteristics optimization of dissimilar welded material.

Keywords Welding · Taguchi optimization · Grey-relational analysis · Multi-performance characteristics

1 Introduction

Welding is unarguably one of the most significant joining processes in metal fabrication technology [1]. Welding in metal entails the use of heat and/or pressure in joining of one or more pieces of metals at a certain temperature with or without a filler material to form a reliable joint. As the need for metal joining increases by the day, several welding techniques have been developed to meet various joint requirements. Quite often, welding processes are classified based on the temperature at which the joining takes place into solid-state welding and fusion welding processes. In solid-state

welding, the welding of the materials takes place at a temperature below the melting points of the materials being joined while in the fusion welding process, the weld joint is brought about by heating the workpieces above their melting temperatures to form a quality joint after solidification.

In several applications, welding of dissimilar metals is required to meet a certain special combination of joint performance as well as reduction of cost in the use of expensive materials [2]. However, welding of dissimilar metals is challenging due to the formation of brittle intermetallic compounds and differences in metallurgical and thermal properties of the metals to be joined. Although solid-state welding processes such as friction stir welding and ultrasonic welding have been adopted in dissimilar welding of metals due to their several advantages such as superior joint strength, thin heat-affected zone and little/no formation of brittle intermetallic compounds [2, 3], their application is limited due to their expensive nature. This makes arc welding processes still relevant in metal fabrication technology. For instance, tungsten inert gas (TIG) welding, an electric

✉ Olawale Samuel Fatoba
drfatobasameni@gmail.com

1   Mechanical Engineering Science, University of Johannesburg, Johannesburg, South Africa

2   Department of Mechanical and Construction Engineering, Northumbria University, Newcastle, UK

arc welding process which involves the use of arc generated a non-consumable tungsten electrode and the workpiece to establish a joint has been deployed as an alternative in dissimilar welding metals due to its lower cost, robustness, manoeuvrability, deep penetration, appreciable deposition rate and reduced weld defects [1, 4–6].

Stainless steel is the choice of material in many engineering applications. This choice is often attributed to its favourable mechanical properties, good corrosion resistance, good weldability and excellent aesthetic appeal. Typical stainless steel applications include but are not limited to automobile parts, rail coach fabrication, structural components in building and bridges, heat exchanger, boilers, aerospace parts, metal gasket in chemical and petrochemical industries and pressure vessels [1, 7–11]. Stainless steels are broadly classified into three subgroups namely austenitic stainless steel, ferritic stainless steel and martensitic stainless steel [1]. Austenitic stainless steel with face-centred cubic structure is the most widely applied stainless steel. This is due to its superior corrosion resistance property compared to ferritic and martensitic stainless steels.

Although stainless steel has low production cost [1], further cost savings can be achieved in fabrication technology by dissimilar welding of stainless steel and lower cost carbon steel. However, the quality of a weld joint is largely dependent on the welding input process parameters [12]. In TIG welding, the input process parameters include the welding current, welding voltage, the gas flow rate, the welding torch nozzle to plate distance and many more. Furthermore, these process parameters must be at their optimal combination to achieve acceptable quality weld joint. This is where optimization techniques become very handy. The most common optimization technique that has attracted the attention of most researchers is the Taguchi optimization method. This method utilizes signal-to-noise ratio (ratio of the mean to the standard deviation) which is a measure of performance in statistics to determine the optimal process parameter setting by exploring the concept of the quadratic loss function. The best combination of the process parameters is then determined by the one with the highest signal-to-noise ratio [12]. However, this traditional method can only be used in the optimization of single objective performance. Fortunately, grey relational analysis can be used for multi-objective/response optimization [13–15]. This analysis can be used to represent the degree of correlation between the two sequences so that the distance between the two factors can be measured discretely. The dissimilar welding of these materials to the best knowledge of authors does not exist in literature. This work is aimed at optimizing the process parameters of TIG dissimilar welding of AISI 316 austenitic stainless steel and AISI 1008 mild steel and their effects on the mechanical properties by the hybrid combination of robust Taguchi method and grey relational analysis.

2 Review of related literature

Several studies have optimized welding process parameters for many weld joint performance characteristics. Natrayan et al. [16], by using the Taguchi method, investigated the optimal welding parameters for maximum tensile strength in TIG welding of AISI 4140 stainless steel. Three welding process parameters, namely, welding current, welding speed and welding wire diameter at 3 levels each, were used to construct L_9-Taguchi orthogonal design. The result revealed that the welding speed had the highest influence on the tensile strength of the weld joint while the optimal combination of the process parameters obtained was welding current at level 1 (250 A) and welding speed and welding wire diameter both at level 3 (5 mm s^{-1} and 3.6 mm respectively). Shanmugasundar et al. [5] used three-level welding current, gas flow rate and nozzle to plate distance to optimize the TIG welding of AISI 304L austenitic stainless steel in terms of the ultimate tensile strength. The maximum ultimate tensile strength obtained from the study was 454.23 MPa. The optimal process parameter was welding current at level 3 (120 A), the gas flow rate at level 1 (10 l.min^{-1}) and nozzle to workpiece distance at level 3 (15 mm). Sridhara et al. [17] optimized the process parameters in TIG welding of Al 7068 aluminium alloy. The maximum tensile strength obtained from the study was 550 MPa. This corresponded with a welding speed of 250 mm min^{-1}, welding current of 40 A and welding voltage of 10 V. Among the three parameters optimized, the welding speed had the highest influence on the tensile strength of the TIG-welded aluminium alloy butt joint with 57.86% contribution. In robotic TIG dissimilar welding of stainless steel 304L and stainless steel 430, Ramana et al. [18] obtained welding current, wire feed rate and welding speed of 180 A, 0.82 mm min^{-1} and 0.08 mm min^{-1} respectively as the optimal combination of the process parameters for maximum impact strength of the weld joint by L_{15} Taguchi orthogonal design. The study observed the wire feed rate to be the most influential parameter in determining the impact strength of the dissimilar joint. Banakis et al. [19] successfully optimized five input process parameters for the desired weld bead geometry and heat-affected zone in pulsed TIG arc additive manufacturing of titanium alloy grade 5 and Inconel 718 using L_{27} Taguchi-inspired approach. The input parameters considered in the study were the main current, background current, delta current, wire feed rate and welding speed all at three levels.

Several types of research have also explored multi-objective response optimization by grey-integrated Taguchi method. Sivakumar and Naik [20] optimized the process parameters in activated flux TIG welding of 6.5-mm-thick Inconel 625 by the hybrid Taguchi method (L_{25} orthogonal array) and grey relational analysis. The welding parameters considered in the study were the

Table 1 Chemical composition of the base materials

Element (wt.%)	Cr	Ni	Mn	Mo	Si	N	C	P	S	Fe
AISI 316	16.4	11.4	2.00	2.6	0.74	0.2	0.07	0.055	0.040	Bal
AISI 1008	~	~	0.220	0.007	0.03	~	0.094	0.002	0.006	Bal

welding current, welding speed and arc gap while the output responses considered were the magnitude of the heat input and the width of the heat-affected zone. The optimal welding current, welding speed and arc gap obtained from the study were 300 A, 75 mm/min and 1 mm respectively. The corresponding heat input and width of the heat-affected zone were 4.212 kJ and 1 mm respectively. Ahmad and Alam [21], by integration grey relational analysis and L_9 Taguchi orthogonal array design, optimized the TIG process parameters for the highest depth of penetration and width of penetration in similar and dissimilar stainless steel 304L and stainless steel 316L TIG weld joint. Prajapati et al. [22] simultaneously obtained the optimal weld bead width, depth of penetration and heat-affected zone of arc-welded A387 low alloy steel by grey-based Taguchi optimization of welding current, welding voltage and gas flow rate. The corresponding values of the process parameters are 135 A, 14 V and 13 l min^{-1} respectively. Furthermore, Avinash et al. [23] simultaneously optimized the ultimate tensile strength, percentage elongation, hardness value, bead width and bead height in pulsed TIG dissimilar welding of austenitic stainless steel 304L and nickel-based superalloy Monel 400 by grey-based Taguchi approach.

3 Experimental procedure

3.1 Selection of base metals

AISI 316 austenitic stainless steel and AISI 1008 mild steel plates having dimension $100 \times 40 \times 6$ mm have been selected as the base materials for TIG welding in butt joint configuration with 2.5-mm gap between the two plates. A 1.6-mm-thick austenitic stainless steel welding wire, ER309L, was used as the filler material. The chemical compositions of the base metals and their mechanical properties are given in Tables 1 and 2 respectively. Crystal argon was selected as the shielding gas.

3.2 Selection of welding process parameters

The selection of the process parameters was based on the literature survey [4, 5, 11, 18, 21]. Welding current, welding voltage and gas flow rate at three levels were selected for L_9 Taguchi orthogonal array. The parameters and their levels are presented in Table 3. The welding of the samples was carried on TIG welding machine, Miller Dynasty (Miller

Table 2 Mechanical properties of the base metals

Base metal	Tensile strength (MPa)	Yield strength (MPa)	Percentage elongation (%)
AISI 316	638.14	498.57	59.68
AISI 1008	395.93	295.95	48.13

Table 3 Welding process parameters and their levels

Symbol	Factors	Units	Level 1	Level 2	Level 3
C	Welding current	Ampere (A)	110	130	150
V	Welding voltage	Voltage (V)	11	12	13
G	Gas flow rate	Litre per minute (l min^{-1})	14	16	18

DX200), in butt joint configuration with double passes (top and bottom).

3.3 Mechanical properties of the welded samples

The quality of the dissimilar weld joints was measured in terms of the ultimate tensile strength, yield strength, percentage elongation and Vickers microhardness of the fusion zone. The tensile test was carried out on 250 KN Zwick/Roell Z250 tensile testing machine with the standard tensile test piece, ASTM-E8. The test was repeated 3 times for each line of the experiment for repeatability. The dimension of the tensile specimen in mm and the tensile testing machine are shown in Fig. 1. The tensile specimens after the tensile test are shown in Fig. 2.

The Vickers microhardness test of the fusion zone of the welded samples was carried out according to ASTM standard E384. The sample size of 20×10 mm was cut off from the welded samples with the weld bead at the centre and was then hot mounted with polyfast resin in such a way as to reveal the transverse section of the weld bead. Mechanical grinding was done with abrasive silicon carbide papers which ranged from 200 to 4000 grits under running water until the surfaces became plane. An indentation force of 500 gf and dwell time of 10 s was chosen for the hardness test. One-millimetre spacing was given between subsequent indentations. Several indentations were taken and

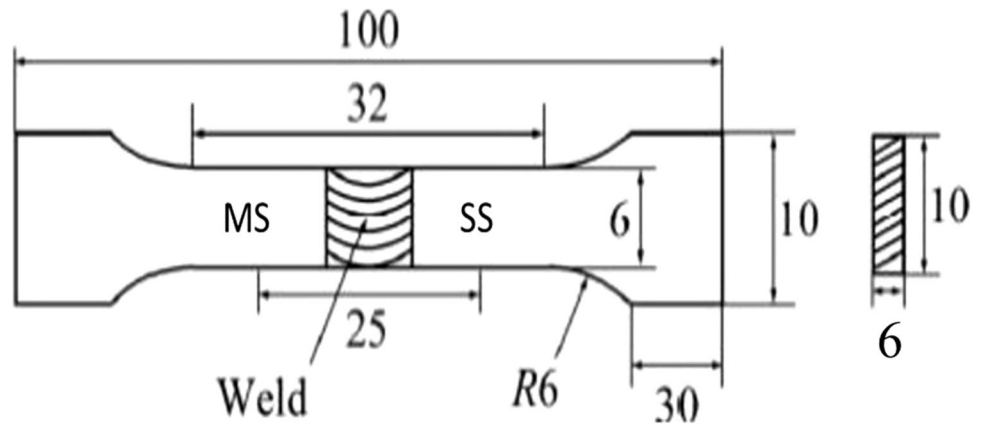**Fig. 1** ASTM-E8 tensile test specimen

Fig. 2 Tensile test samples after the tensile test

the average taken as the Vickers microhardness value of the fusion zone.

3.4 Taguchi optimization method

Taguchi optimization approach which was developed by Japanese engineer and statistician. The method enhances the quality and at the same time reduces cost [12]. It is a robust method because it enhances the response as it reduces its sensitivity to causes of variability and still does not eliminate the causes. The process factors which are known and can be controlled are called the signal factors while those which are not within the control of the process manager are termed as the noise factors. There are three standard signal-to-noise (S/N) ratios generally used in Taguchi optimization, namely, nominal-is-best (NB), smaller-the-better (SB) and larger-the-better (LB), and this depends on the desired response. These are illustrated in Eqs. (i–iii). This study adopted L_9 Taguchi orthogonal array to optimize the welding current, welding voltage and gas flow rate in terms of the weld joint ultimate tensile strength (UTS), yield strength (YS), percentage elongation (%EL) and fusion zone Vickers microhardness (FZ_{HV}). Each parameter was considered at three levels as shown in Table 3. The L_9 Taguchi orthogonal array

Table 4 L_9 Taguchi orthogonal array

Exp no	Welding current (A)	Welding voltage (V)	Gas flow rate (l min^{-1})
1	110	11	14
2	110	12	16
3	110	13	18
4	130	11	16
5	130	12	18
6	130	13	14
7	150	11	18
8	150	12	14
9	150	13	16

based on the parameters chosen in this study is shown in Table 4 while the corresponding output responses considered in this study are presented in Table 5.

1. Signal-to-noise ratio for nominal-is-best:

$$\eta = 10 \, log \frac{1}{n} \sum_{i=1}^{n} \frac{\mu^2}{\sigma^2} \quad (1)$$

2. Signal-to-noise ratio for smaller-the-better:

Table 5 Experimental results

Exp no	Welding current (A)	Welding voltage (V)	Gas flow rate (l min^{-1})	UTS (MPa)	YS (MPa)	%EL (%)	FZ$_{HV}$ (HV)
1	110	11	14	463.68	334.47	30.50	289.52
2	110	12	16	453.94	340.53	28.51	386.13
3	110	13	18	485.64	362.73	29.15	285.83
4	130	11	16	440.22	331.16	27.56	299.51
5	130	12	18	433.28	366.80	17.55	208.35
6	130	13	14	418.09	339.40	29.17	291.93
7	150	11	18	468.66	341.51	22.75	325.33
8	150	12	14	414.22	293.93	26.91	347.95
9	150	13	16	415.88	351.37	27.32	335.25

$$\eta = -10 \, log \frac{1}{n} \sum_{i=1}^{n} y_i^2 \tag{2}$$

3. Signal-to-noise ratio for larger-the-better:

$$\eta = -10 \, log \frac{1}{n} \sum_{i=1}^{n} \frac{1}{y_i^2} \tag{3}$$

where η is the signal-to-noise ratio, n is the number of experiments, μ is the mean of the signal-to-noise ratio, σ is the standard deviation, and y_i is the corresponding response. The combination of the parameters that give the highest signal-to-noise ratio is seen as the optimal setting [12].

3.5 Grey-Relational Analysis (GRA)

The grey-relational analysis follows four basic steps. The four steps are as follows [22]:

1. Normalization of the data

Depending on the respective signal-to-noise ratio, the equations for normalization of the data are given in Eqs. (4–5) [1].

(a) For smaller-the-better
This applies where a smaller error in the response is to be achieved. The equation for normalization is

$$X_{ij} = \frac{Y_{ijmax} - Y_{ij}}{Y_{ijmax} - Y_{ijmin}} \tag{4}$$

(b) For larger-the-better
This applies where a greater value of the response needs to be achieved. The equation for normalization here is

$$X_{ij} = \frac{Y_{ij} - Y_{ijmin}}{Y_{ijmax} - Y_{ijmin}} \tag{5}$$

where X_{ij} is the normalized signal-to-noise ratio, Y_{ij} is the corresponding S/N ratio obtained from Taguchi, and Y_{ijmax} and Y_{ijmin} are respectively the obtained maximum and the minimum Taguchi S/N ratios.

2. Calculation of the deviation sequence (DS)

Table 6 S/N ratios of the response variables

| Exp no	Welding current (A)	Welding voltage (V)	Gas flow rate (l min^{-1})	UTS (MPa)	YS (MPa)	%EL (%)	FZ$_{HV}$ (HV)
1	110	11	14	53.32437	50.48714	29.68600	49.23357
2	110	12	16	53.13997	50.64311	29.09994	51.73467
3	110	13	18	53.72629	51.19167	29.29277	49.12216
4	130	11	16	52.87340	50.40076	28.80558	49.52823
5	130	12	18	52.73537	51.28859	24.88554	46.37587
6	130	13	14	52.42540	50.61424	29.29873	49.30557
7	150	11	18	53.41716	50.66807	27.13963	50.24648
8	150	12	14	52.34462	49.36488	28.59827	50.83034
9	150	13	16	52.37936	50.91529	28.72961	50.50738
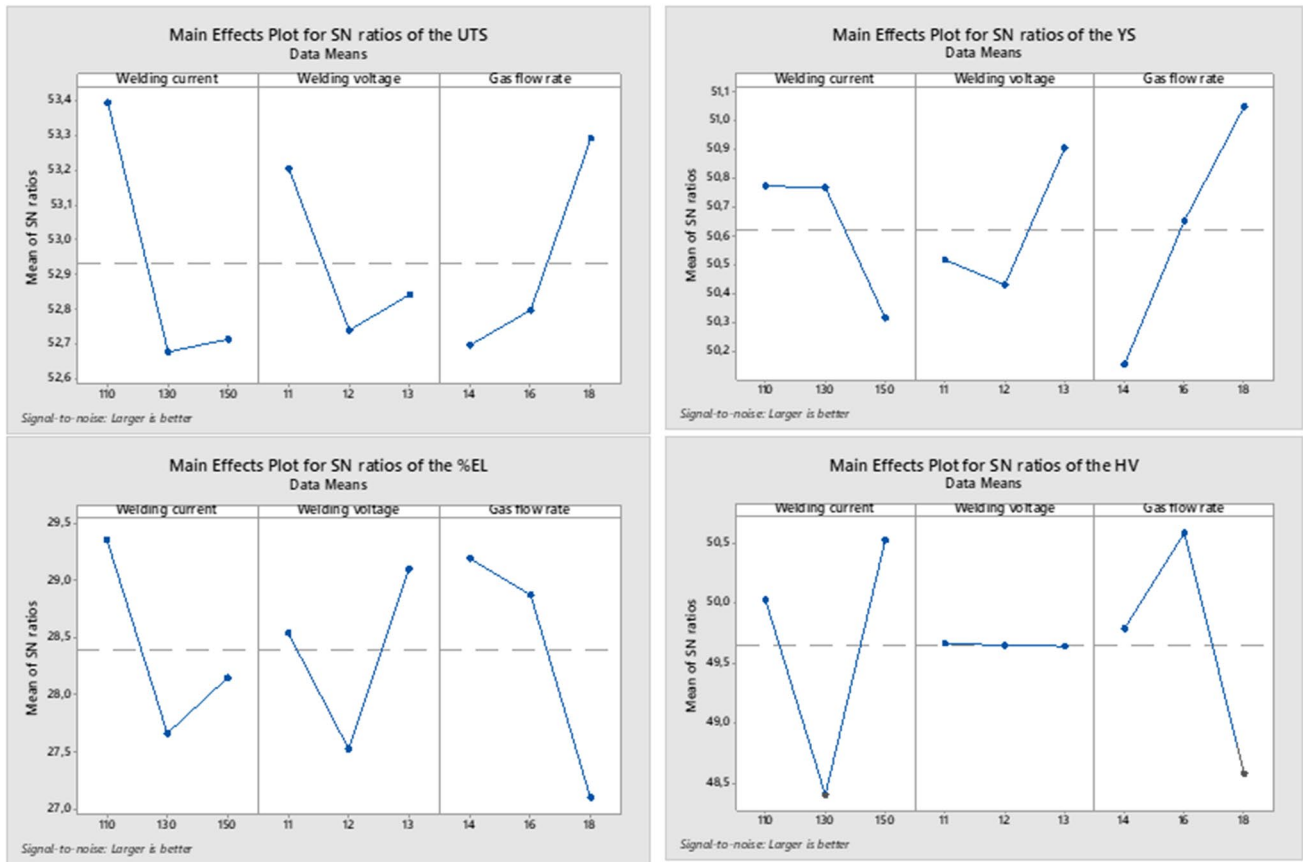
Fig. 3 Main effect plots of the response variables vs the welding parameters

This step involves the calculation of the absolute difference from the normalized sequence. This is given by Eq. (6) [24] as

$$\Delta_{ij} = \left| Y_{ijmax} - Y_{ij} \right|$$ (6)

where Δ_{ij} is the deviation sequence, Y_{ijmax} is the maximum value obtained after normalization, and Y_{ij} is the corresponding reference sequence.

3. Calculation grey-relational coefficient (GRC)

This is done to relate the ideal to the normalized data. This is calculated using the Eq. (7):

$$\delta_{ij} = \frac{\Delta_{min} + \varepsilon.\Delta_{max}}{\Delta_{ij} + \varepsilon.\Delta_{max}}$$ (7)

where δ_{ij} is the grey-relational coefficient, Δ_{ij} is the reference deviation sequence, ε is the distinguishing coefficient always taken as 0.5, Δ_{min} and Δ_{max} are the minimum and maximum deviation sequence.

4. Calculation of the grey-relational grade (GRG)

Table 7 Normalized S/N ratios of the response variables

Exp no	Welding current (A)	Welding voltage (V)	Gas flow rate (l min⁻¹)	UTS (MPa)	YS (MPa)	%EL (%)	FZ$_{HV}$ (HV)
1	110	11	14	0.70910	0.58339	1.00000	0.53327
2	110	12	16	0.57564	0.66446	0.87792	1.00000
3	110	13	18	1.00000	0.94962	0.91809	0.51248
4	130	11	16	0.38271	0.53848	0.81660	0.58826
5	130	12	18	0.28281	1.00000	0.00000	0.00000
6	130	13	14	0.05846	0.64945	0.91933	0.54671
7	150	11	18	0.77626	0.67744	0.46956	0.72229
8	150	12	14	0.00000	0.00000	0.77341	0.83124
9	150	13	16	0.02514	0.80595	0.80077	0.77098

Table 8 Deviation sequences of the response variables

Exp no	Welding current (A)	Welding voltage (V)	Gas flow rate (l min^{-1})	UTS (MPa)	YS (MPa)	%EL (%)	FZ$_{HV}$ (HV)
1	110	11	14	0.29090	0.41661	0.00000	0.46673
2	110	12	16	0.42436	0.33554	0.12208	0.00000
3	110	13	18	0.00000	0.05038	0.08191	0.48752
4	130	11	16	0.61729	0.46152	0.18340	0.41174
5	130	12	18	0.71719	0.00000	1.00000	1.00000
6	130	13	14	0.94154	0.35055	0.08067	0.45329
7	150	11	18	0.22374	0.32256	0.53044	0.27771
8	150	12	14	1.00000	1.00000	0.22659	0.16876
9	150	13	16	0.97486	0.19405	0.19923	0.22902

Table 9 Grey-relational coefficient of the response variables

Exp no	Welding current (A)	Welding voltage (V)	Gas flow rate (l min^{-1})	UTS (MPa)	YS (MPa)	%EL (%)	FZ$_{HV}$ (HV)
1	110	11	14	0.63219	0.54549	1.00000	0.51721
2	110	12	16	0.54092	0.59842	0.80375	1.00000
3	110	13	18	1.00000	0.90846	0.85923	0.50632
4	130	11	16	0.44751	0.52001	0.73163	0.54840
5	130	12	18	0.41078	1.00000	0.33333	0.33333
6	130	13	14	0.34685	0.58786	0.86107	0.52450
7	150	11	18	0.69086	0.60786	0.48523	0.64291
8	150	12	14	0.33333	0.33333	0.68815	0.74766
9	150	13	16	0.33902	0.72041	0.71507	0.68585

This is the final step in a grey-relational generation. It is obtained by taking the average of the grey-relational coefficients. The equation for calculating grey-relational grade is given by Eq. (8). The higher the value of GRG, the closer the corresponding parameter setting is to the optimum setting [24]:

$$\gamma_{ij} = \frac{1}{n} \sum_{k=1}^{n} \delta_{ij} \tag{8}$$

where γ_{ij} is the grey-relational grade, n is the number of response variables, and δ_{ij} is the grey-relational coefficient.

4 Results and discussion

The results of the experiment and their analysis are presented in this section.

4.1 Taguchi optimization results and analysis

The ultimate tensile strength, yield strength, percentage elongation and Vickers microhardness of the fusion zone as obtained from the experiment are presented in Table 5 while their signal-to-noise ratios and main effects plots against the input process parameters are given in Table 6

and Fig. 3 respectively. From Table 5, it can be observed that the maximum ultimate tensile, yield strength, percentage elongation and Vickers microhardness were 485.64 MPa, 366.80 MPa, 30.50% and 386.13 HV respectively. These corresponded to experiment numbers 3, 5, 1 and 2 respectively. From the main effect plots of each response variable against the input process parameters, as shown in Fig. 3, the optimum setting for the ultimate tensile strength is welding current at level 1, welding voltage at level 1 and gas flow rate at level 3 (110 A, 11 V and 18 l min^{-1}). For the yield strength, the optimum setting is

Table 10 Parameter setting, grey-relational grade and rank

Exp no	Welding current (A)	Welding voltage (V)	Gas flow rate (l min^{-1})	GRG	Rank
1	110	11	14	0.67372	3
2	110	12	16	0.73577	2
3	110	13	18	0.81850	1
4	130	11	16	0.56189	7
5	130	12	18	0.51936	9
6	130	13	14	0.58007	6
7	150	11	18	0.60671	5
8	150	12	14	0.52562	8
9	150	13	16	0.61509	4

Fig. 4 Main effect plot of the GRG vs the welding parameters
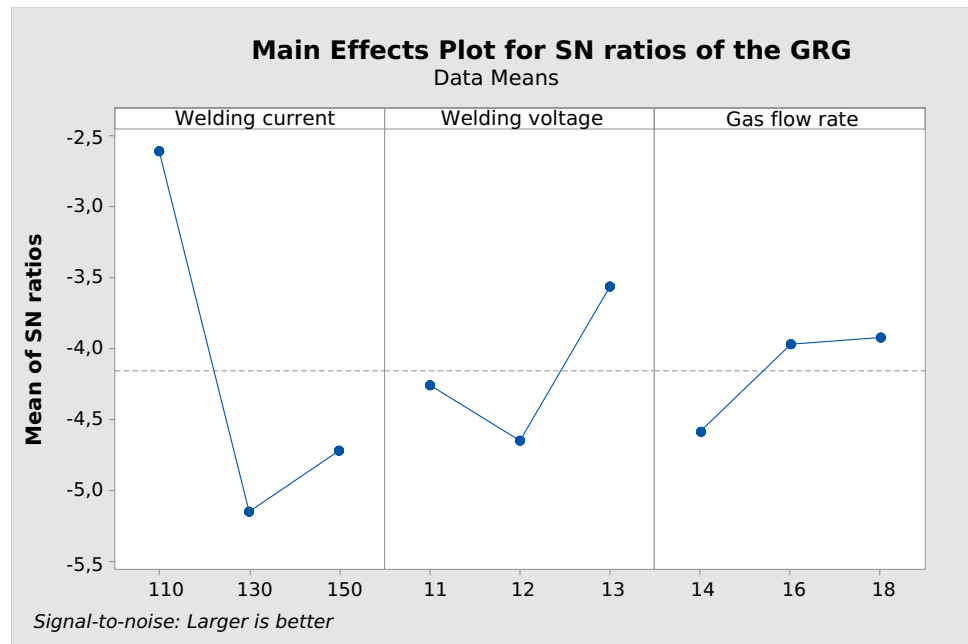
welding current at level 1, welding voltage at level 3 and gas flow rate at level 3 (110 A, 13 V and 18 l min^{-1}). The optimum setting for the percentage elongation is welding current at level 1, welding voltage at level 3 and gas flow rate at level 1 (110 A, 13 V and 14 l min^{-1}) and finally the corresponding optimum setting for the Vickers microhardness is welding current at level 3, welding voltage at level 1 and gas flow rate at level 2 (150 A, 11 V and 16 l min^{-1}).

4.2 Grey-integrated Taguchi analysis

As can be observed from Section 4.1 in the Taguchi analysis of each of the response variable, the different optimum setting was obtained for each of the response variables. Hence, to obtain the unique optimum setting for the combined response variables, the grey-relational analysis was carried out following the standard procedure enumerated in Section 3. The normalized S/N ratios, deviation sequences, grey-relational coefficients and grey-relational grades of the response variables are displayed in Tables 7, 8, 9 and 10 respectively. The maximum grey-relational grade of 0.81850 from Table 10 was obtained at experiment number 3 corresponding to welding current, welding voltage and gas flow rate of 110 A, 13 V and 18 l min^{-1} respectively. The main effect plot of the grey-relational grade (GRG) against the input process parameters and the analysis of variance (ANOVA) are presented in Fig. 4 and Table 11 respectively.

From Fig. 4, the optimum setting for all the performance characteristics considered in this work is welding current at level 1 (110 A), welding voltage at level

Table 11 ANOVA of the GRG vs the welding parameters

Source	DF	Seq SS	Contribution	Adj SS	Adj MS	F-value	p-value	Significance
Current	2	0.062166	78.15%	0.062166	0.031083	24.4	0.039	Significant
Voltage	2	0.00971	12.21%	0.009710	0.004855	3.81	0.208	Non-significant
Gas flow rate	2	0.005119	6.44%	0.005119	0.00256	2.01	0.332	Non-significant
Error	2	0.002548	3.20%	0.002548	0.001274			
Total	8	0.079543	100.00%					

Table 12 Results of the confirmatory test

Optimal setting						
Welding current (A)	Welding voltage (V)	Gas flow rate (l min^{-1})	UTS (MPa)	YS (MPa)	%EL (%)	FZ$_{HV}$ (HV)
110	11	18	493.29	395.38	31.35	390.52

3 (13 V) and gas flow rate at level 3 (18 l min^{-1}). The ANOVA analysis performed at 95% confidence level as shown in Table 11 shows that the welding current with 78.15% contribution, and p-value of 0.039 was the most significant process parameter followed by the welding voltage and then the gas flow rate for the multi-objective performance of the dissimilar weld joint.

4.3 Confirmatory test

The confirmatory test was conducted to validate the optimization process with the optimal parameters. The results of the confirmatory test are shown in Table 12. From the results of the confirmatory test, it can be observed that higher values of the response variables were obtained at the optimal parameters. This validates the grey-integrated Taguchi optimization carried out in this work.

5 Conclusions

The grey-integrated Taguchi optimization of multi-performance characteristics of TIG butt dissimilar weld joint of AISI 1008 and AISI 316 has been demonstrated in this work. The grey-relational analysis was used to convert multi-performance objectives of the welded samples into a single-performance objective. The following conclusions can be deduced from the study:

- At optimized parameters of welding current at level 1 (110 A), welding voltage at level 1 (11 V), and gas flow rate at level 3 (18 l min^{-1}), the mechanical properties of the TIG butt dissimilar weld joint of AISI 1008 mild steel and AISI 316 austenitic stainless steel were enhanced based on grey-integrated Taguchi optimization technique.
- The welding current with 78.15% contribution and p-value of 0.039 was the most significant process parameter. This shows the influence of the welding current on the mechanical property enhancement.
- Higher mechanical properties at optimized process parameters could have occurred due to the mixed structure of austenite and ferrite or other particles in the weld metal.
- The multi-objective optimization was validated with optimal parameters. From the results of the confirmatory test, it can be observed that higher values of the response variables were obtained at the optimal parameters. This validates the grey-integrated Taguchi optimization carried out in this work.

Declarations

References

1. BalaramNaik A, Chennakeshava Reddy A (2018) Optimization of tensile strength in TIG welding using the Taguchi method and analysis of variance (ANOVA). Therm Sci Eng Prog 8:327–339. https://doi.org/10.1016/j.tsep.2018.08.005. (Elsevier)

2. Paventhan R, Lakshminarayanan PR, Balasubramanian V (2011) Fatigue behaviour of friction welded medium carbon steel and austenitic stainless steel dissimilar joints. Mater Design 32:1888–1894. https://doi.org/10.1016/j.matdes.2010.12.011. (Elsevier Ltd)

3. Argade GR, Shukla S, Liu K, Mishra RS (2018) Friction Stir lap welding of stainless steel and plain carbon steel to enhance corrosion properties. J Mater Process Tech 259:259–269. https://doi.org/10.1016/j.jmatprotec.2018.04.048. (Elsevier)

4. Kant R, Mittal C, Kumar BS, Rana M, Kumar R. Kumar (2018) Fabrication and characterization of weldments AISI 304 and AISI 316 used in industrial applications. Mater Today: Proceedings 5(9):18475–18481

5. Shanmugasundar G, Karthikeyan B, Vignesh V (2019) Optimization of process parameters in TIG welded joints of AISI 304L-austenitic stainless steel using Taguchi's experimental design method. Material Today: Proceedings 16:1188–1195

6. Silwal B, Santangelo M (2018) Effect of vibration and hot-wire gas tungsten arc (GTA) on the geometric shape. J Mater Process Tech 251:138–145. https://doi.org/10.1016/j.jmatprotec.2017.08.010. (Elsevier)

7. Bu Y, Gardner L (2018) Local stability of laser-welded stainless steel I-sections in bending. J Constr Steel Res 148:49–64. https://doi.org/10.1016/j.jcsr.2018.05.010

8. Yan S, Shi Y, Liu J, Ni C (2019) Effect of laser mode on microstructure and corrosion resistance of 316L stainless steel weld joint. Opt Laser Technol 113:428–436. https://doi.org/10.1016/j.optlastec.2019.01.023. (Elsevier Ltd)

9. Keskitalo M, Sundqvist J, Mäntyjärvi K, Powell J, Kaplan AFH (2015) The influence of shielding gas and heat input on the mechanical properties of laser welds in ferritic stainless steel, physics Procedia, vol 78. Elsevier B.V., p 222–229. https://doi.org/10.1016/j.phpro.2015.11.032

10. Wu SK, Zheng K, Zou JL, Jiang F, Han XH (2018) A study of the behavior and effects of nitrogen take-up from protective gas shielding in laser welding of stainless steel. J Manuf Process 34:477–485. https://doi.org/10.1016/j.jmapro.2018.06.031

11 Mohammad H, Tayebi M (2018) Comparative study of AISI 304L to AISI 316L stainless steels joints by TIG and Nd : YAG laser welding. J Alloys Compd 767:112–21. https://doi.org/10.1016/j.jallcom.2018.06.302. (Elsevier B.V)

12. Ghosh N, Pal PK, Nandi G (2016) Parametric optimization of MIG welding on 316L austenitic stainless steel by grey-based Taguchi Method. Procedia Technology 25(2016):1038–1048. https://doi.org/10.1016/j.protcy.2016.08.204

13. Çaydaş U, Hasçalik A (2008) Use of the grey relational analysis to determine optimum laser cutting parameters with multi-performance characteristics. Opt Laser Technol 40:987–994. https://doi.org/10.1016/j.optlastec.2008.01.004

14. Suji D, Adesina A, Mirdula R (2021) Optimization of self-compacting composite composition using Taguchi-Grey relational analysis. Materialia 15(101027). https://doi.org/10.1016/j.mtla.2021.101027

15. Singh M, Singh S (2021) Multiple response optimization of ultrasonic assisted electric discharge machining of Nimonic 75: a Taguchigrey relational analysis approach. Mater Today: Proc 45:4731–4736. https://doi.org/10.1016/j.matpr.2021.01.173

16. Natrayan L, Anand R, Santhosh Kumar S (2020) Optimization of process parameters in TIG welding of AISI 4140 stainless steel using taguchi technique. Mater Today: Proc. https://doi.org/10.1016/j.matpr.2020.07.150. (Elsevier Ltd)

17. Shiva naga sathwik sridhara, Sree chandra siddhardha Allada, Sharmi Sai PV, Spandana Banala, Ram Subbiah, Marichamy S (2020) Tensile strength performance and optimization of Al 7068 using TIG welding process. Mater Today: Proceed, Elsevier Ltd. https://doi.org/10.1016/j.matpr.2020.09.481

18. Ramana MV, Kumar BVRR, Krishna M, Rao MV, Kumar VS (2020) Optimization and influence of process parameters of dissimilar SS304L - SS430 joints produced by robotic TIG welding. Mater Today: Proc 23:479–482. https://doi.org/10.1016/j.matpr.2019.05.388. (Elsevier Ltd)

19. Benakis M, Costanzo D, Patran A (2020) Current mode effects on weld bead geometry and heat affected zone in pulsed wire arc additive manufacturing of Ti-6-4 and Inconel 718. J Manuf Proc 60:61–74. https://doi.org/10.1016/j.jmapro.2020.10.018. (Elsevier Ltd)

20. Sivakumar J, Nanda Naik K (2019) Optimization of weldment in bead on plate welding of nickel based superalloy using activated flux tungsten inert gas welding (A-TIG). Mater Today: Proc 27:2718–2723. https://doi.org/10.1016/j.matpr.2019.11.327. (Elsevier Ltd)

21. Ahmad A, Alam S (2019) Integration of RSM with grey based Taguchi method for optimization of pulsed TIG welding process parameters. Mater Today: Proc 18:5114–5127. https://doi.org/10.1016/j.matpr.2019.07.508. (Elsevier Ltd)

22. Prajapati V, Dinbandhu, Vora JJ, Das S, Abhishek K (2020) Study of parametric influence and welding performance optimization during regulated metal deposition (RMD^{TM}) using grey integrated with fuzzy Taguchi approach. J Manuf Process 54:286–300. https://doi.org/10.1016/j.jmapro.2020.03.017. (Elsevier)

23. Avinash S, Balram Y, Sridhar Babu B, Venkatramana G (2019) Multi-Response optimization of pulse TIG welding process parameters of welds AISI 304 and Monel 400 using grey relational analysis. Mater Today: Proc 19:296–301. https://doi.org/10.1016/j.matpr.2019.07.211. (Elsevier Ltd)

24. Prabakaran MP, Kannan GR (2019) Optimization of laser welding process parameters in dissimilar joint of stainless steel AISI316 / AISI1018 low carbon steel to attain the maximum level of mechanical properties through PWHT. Opt Laser Technol 112:314–322. https://doi.org/10.1016/j.optlastec.2018.11.035. (Elsevier Ltd)